Horizontal thermal convection in a shallow cavity: oscillatory regimes and transition to chaos

Edoardo Bucchignani
Centro Italiano Ricerche Aerospaziali, Capua, Italy, and
Daniela Mansutti
Istituto per le Applicazioni del Calcolo/CNR, Roma, Italy

Received July 1999
Accepted August 1999

Keywords *Natural convection, Fluids, Numerical analysis*

Abstract *We develop a numerical analysis of the buoyancy driven natural convection of a fluid in a three dimensional shallow cavity (4 · 1 · 1) with a horizontal gradient of temperature along the larger dimension. The fluid is a liquid metal (Prandtl number equal to 0. 015) while the Grashof number (Gr) varies in the range 100,000-300,000. The Navier-Stokes equations in vorticity-velocity formulation have been integrated by means of a linearized fully implicit scheme. The evaluation of fractal dimension of the attractors in the phase space has allowed the detection of the chaotic regime. The Ruelle-Takens bifurcation sequence has been observed as mechanism for the transition to chaos: the quasi periodic regime with three incommensurate frequencies is the instability mechanism responsible for the transition to chaos. Physical experiments confirm the existence of this scenario.*

1 Introduction

Buoyancy driven natural convection of liquid metals has relevance in a wide range of engineering and industrial applications such as crystal growth, glass manufacturing, welding and material processing. In many cases the liquid material is enclosed in a rigid parallelepipedic box with a horizontal gradient of temperature which induces the convective flow.

It is well known that the main parameters which drive the phenomenon are the Prandtl number (*Pr*) and the Grashof number (*Gr*). Liquid metal buoyancy driven convection (in the absence of surface tension driven flow) at low values of *Gr* is laminar and steady. However, as *Gr* is increased the convective flow is known to become time-dependent and oscillatory (Roux, 1990). Experimental evidence of this phenomenon in molten gallium is given by Hurle *et al.* (1974). Experimental results by Hart (1972), Hung and Andereck (1990) and Wang *et al.* (1990) also clearly show that there is a transition from steady to unsteady flow. This behaviour can have a serious influence on the relevant applications. For instance, in the Czochralski or Bridgman technique for the artificial crystal growth, the melt material undergoes convective motions due to the difference between liquid and solid temperature. The oscillatory instabilities of the melt

This work has been performed within the project 1996-97 "Modelli matematici, analisi sperimentale e numerica di alcuni aspetti della cristallizzazione da fuso in microgravitá", funded by Italian Space Agency. CIRA is also gratefully acknowledged for providing computational resources for parallel simulations.

flow are the main reason of in homogeneities in the final product (Hurle, 1983). In the absence of gravity, it is also possible to have convective instabilities driven by surface tension effects. This problem has been extensively studied by Lebon (1984) as well as others.

Many successful efforts have been done for a detailed study of two dimensional problems (careful studies are described in Winters (1988), Pulicani *et al.* (1990), Ben Hadid and Roux (1990) and many others). From a rough comparison with the mathematical and numerical studies of the Benard problem (vertical thermal convection), there is a fundamental difference, that is the absence for the present problem of an analytical physically meaningful solution to start the flow bifurcation pattern. Actually pure conduction is here unstable whereas in the Benard case it is the exact solution from which departs the one-cell flow configuration (first bifurcation point) (Drazin and Reid, 1985). Then in the Benard flow, linear and nonlinear stability analysis have been based on an unambiguous startup, whilst the results by stability analysis of the horizontal thermal convection flow are obtained around some initial approximated solution calculated through asymptotic techniques (Cormack *et al.*, 1974; Georgescu and Mansutti, 1998; 1999). Other mathematical treatments carefully developed can be found in Gershuni *et al.* (1992), where the hypothesis is quite restrictive. This picture suggests that for this flow the most appropriate studying tool is the numerical simulation. However for the inadequacy of computational resources the study of three dimensional flows has been limited again. Only few results are available on some steady flow configurations due to combined buoyancy and thermocapillary effects (Berhnia *et al.*, 1995; Gianji *et al.*, 1998).

The aim of this work is the study of the flow in a shallow three dimensional box $(4 \cdot 1 \cdot 1)$, whose smaller vertical walls are rigid, isothermal and held at different values of temperature, while the other walls are rigid and insulated (Figure 1). The box is filled with a liquid metal (Prandtl number equal to 0. 015).

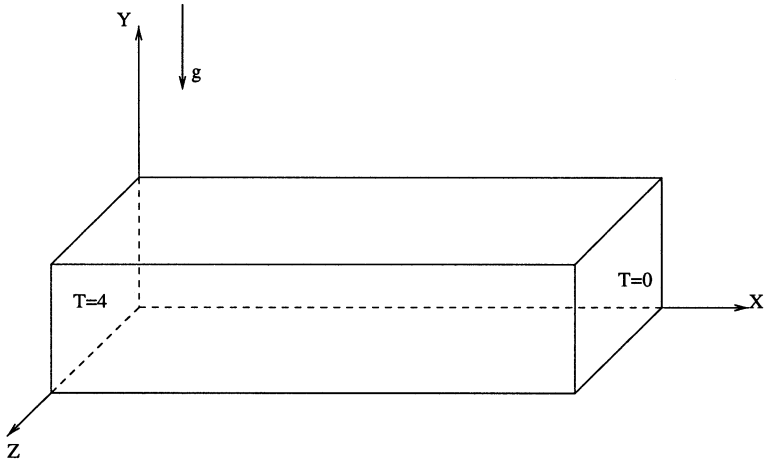

Figure 1.
Scheme of the computational domain

The Grashof number has been varied in a wide range, in order to observe the transition from steady state to the periodic regime, and from this to the non-periodic one (chaos).

Although there is not a scientific definition of chaos, our common experience is related with some of its typical properties, the most representative of which is the difficulty in the predictability of the results: a chaotic system loses the memory of itself or, in other words, the knowledge of the status of the system for a finite time interval does not allow us to foresee its further evolution. The power spectrum of a chaotic regime is continuous. A real difficulty is that a Fourier spectrum which looks continuous cannot be automatically attributed to a chaotic signal, because it can be also representative of a quasi-periodic signal with a very high number of frequencies (white noise). In the first case, a completely deterministic description of the system can be given because chaos, although unpredictable, is governed by a set of well known equations (Lorenz, 1963): this means that two phase trajectories (representative of the evolution of a system) never can intersect themselves or, in other words, a chaotic system, starting from a fixed state, can evolve in a univocal way. On the other hand, if we are dealing with a white noise signal, only a probabilistic insight can be achieved with the current state of knowledge. Therefore, the Fourier analysis is not able to characterize a chaotic signal; for this reason, a non linear dynamics technique, such as the evaluation of fractal dimension of the attractors in the phasespace, has also been used in order to quantify and detect the chaotic state of the system.

Even if a lot of work has also been done, the transition to chaos still remains an open problem and several transition mechanisms have been detected, both numerically and experimentally (Gollub and Benson, 1980; Guzman and Amon, 1996; Bucchignani and Stella, 1998). In this work, at $Gr = 205,000$ the first Hopf bifurcation is observed when a periodic regime stems from a steady one; then one of the most common sequences of bifurcations has been detected and deeply analyzed: the Ruelle-Takens route, involving two Hopf bifurcations, leading respectively to a quasi periodic regime with two frequencies at $Gr = 206,000$ and from this to a quasi periodic regime with three frequencies $Gr = 215,000$. This last regime, according to the Newhouse-Ruelle-Takens theorem (Newhouse *et al.*, 1978), is not stable and immediately degenerates to a chaotic flow. It is worth noting that all the bifurcations have been observed in a limited range of values of Gr, $205,000 \leq Gr \leq 215,000$ highlighting a sudden transition from the steady state to chaos.

The study has been conducted by direct numerical simulations, using a fully implicit parallel code based on the vorticity-velocity formulation of the Navier-Stokes equations, assuming the Boussinesq approximation to be valid. The mathematical model is described in section 2. The numerical discretization and the solution method are explained in section 3. A finite difference scheme has

been adopted and a preconditioned Bi-CGSTAB algorithm is used to solve the linear systems arising from the discretization (van der Vorst, 1992). In section 4 results are presented and discussed.

2 Mathematical formulation

2. 1 Governing equations

The Navier-Stokes equations for an incompressible Newtonian fluid with the Boussinesq approximation are formulated in terms of vorticity ω velocity $\mathbf{u} = (u, v, w)$ and temperature θ. The following non-dimensional form is adopted:

$$\frac{\partial \omega}{\partial t} + Gr^{1/2}\nabla \times (\omega \times \mathbf{u}) = \nabla^2 \omega - Gr^{1/2}\nabla \times \left(\theta \frac{\mathbf{g}}{|g|}\right) \tag{1}$$

$$\nabla^{\mathbf{2}}\mathbf{u} = -\nabla \times \omega \tag{2}$$

$$Pr\frac{\partial \theta}{\partial t} + Pr \cdot Gr^{1/2}(\mathbf{u} \cdot \nabla)\theta = \nabla^2 \theta. \tag{3}$$

The vorticity ω is defined as usual:

$$\omega = \nabla \times \mathbf{u} \tag{4}$$

We remember that the non-dimensional parameters Gr and Pr are defined as:

$$Gr = \frac{g\beta \Delta T H^3}{\nu^2}, Pr = \frac{\nu}{\kappa}$$

in which g is the gravitational acceleration, β is the coefficient of thermal expansion, H is the height of the box, ΔT is the temperature difference between hot and cold walls, κ the thermal diffusivity and ν is the kinematic viscosity. The underlying reference quantities are: $\mathbf{u}^* = Gr^{1/2}\nu/H$ (velocity reference), $t^* = H^2/\nu$ (time reference), $l^* = Gr^{1/2}H$ (length reference) and $\theta^* = \Delta T$ (temperature reference).

The standard conservative form is adopted for the convective terms in the vorticity transport equation in order to conserve exactly the mean vorticity as prescribed by the Stokes theorem. This contributes to avoiding possible numerical inconsistencies. The vertical direction has been assumed coincident with the *y* axis.

2. 2 Boundary conditions

The domain considered is a three-dimensional box whose dimensions are: $L_x = 4, H_y = 1, L_z = 1$ (see Figure 1). The formulation used here allows a very simple way of applying the boundary conditions:

- the boundary condition associated with equation (1) is the vorticity definition (4) written on the boundary. Due to the time discretization scheme used, this boundary condition is updated and enforced at each

current time step. This procedure contributes to the correct coupling between the kinematic and the dynamic parts of the problem;

- the boundary conditions associated with the elliptic velocity equations (2) are the velocity components u, v and w enforced to be zero on the walls.
- the boundary conditions associated with the energy equation are:

$$\theta = 0 \qquad \{x = 0$$

$$\theta = 1 \qquad \{x = L_x$$

$$\frac{\partial \theta}{\partial n} = 0 \begin{cases} y = 0 \\ y = H_y \\ z = 0 \\ z = L_z \end{cases}$$

3 Solution procedure

3.1 Numerical model

The governing equations (1), (2), (3) together with the proper boundary conditions are discretized by using finite difference approximations. Spatial derivatives are discretized on a uniform mesh through central second-order differences while time derivatives are discretized through three-point second-order backward differences.

By the chosen finite difference schemes, the discrete model ensures maximum accuracy by a staggered variable location. For this purpose the MAC scheme, originally built for the $(\mathbf{u}, \theta)$ formulation by Harlow and Welch (1965), has been adapted to the present $(\mathbf{u}, \omega, \theta)$ formulation. In general when each velocity component is evaluated at the middle of the faces of the computational cell which are orthogonal, the mass conservation law at the discrete level can be satisfied up to meet the round-off error. In a similar way, by evaluating the vorticity components at the mid-point of the edges of the computational cell which are parallel, the natural property of solenoidality of the vorticity can be met at the discrete level up to round off error. Furthermore, in our model staggering of the variables allows to discretize the equation (2) in a "clean" way without any need of averaging. On the contrary, in discretizing the equation (1), averaging is necessary for the treatment of the advective term $\nabla \times (\omega \times \mathbf{u})$, where the product $\omega \times \mathbf{u}$ is here averaged in the whole (Guj and Stella, 1993). In this way the resulting discrete equation is consistent with the implicit property of solenoidality of the vorticity field expressed in discrete form.

The computation of the numerical solutions has been performed by a time dependent algorithm. A true transient procedure requires particular care when used together with the vorticity-velocity formulation. In fact the

continuity equation is imposed only in an implicit way by dropping the term $\nabla \dot{\mathbf{u}}$ in the equations (1, (2), (3) so that mass conservation and definition of vorticity could be violated if good coupling among the full set of the equations is not ensured. Then the time integration has been executed by means of a fully implicit numerical-scheme that has been afterwards linearized through the "frozen coefficients" technique (Stella and Bucchignani, 1996).

In this way at each time step our original system of partial differential equations gives rise to a large linear system of equations of the type

$$\mathbf{A}x = b$$

where $\mathbf{x}$ is the unknown vector and $\mathbf{b}$ is the known vector. The coefficient matrix $\mathbf{A}$ has a large sparse structure. The solution of this linear system via a direct method is not recommended due to the size of the problem, so that an iterative procedure has been adopted: a variant of preconditioned conjugate gradient is proposed. This approach has the advantage to allow a great flexibility in writing the discretized form of numerical model. We have used a parallel implementation of the Bi-CGSTAB algorithm (van der Vorst, 1992; Bucchignani and Stella, 1995), because of its numerical stability and speed of convergence. Although, from a theoretical point of view, iterative methods can be used without preconditioning the linear systems of equations, the use of a preconditioning technique is, in many practical applications, essential to fulfil the convergence and stability requirements of the iterative procedure itself. The aim of the preconditioner is to convert the original linear system to an equivalent but better-conditioned system. This consists of finding a real matrix C such that the new linear system

$$C^{-1}\mathbf{A}x = C^{-1}b$$

has (by design) better convergence and stability characteristics than the original system. It is obvious that the matrix C must be chosen carefully: it should be close to the inverse of A, but easy to invert to avoid increased computational cost. The ILU factorization is one of the most widely used preconditioners: C is defined as the product LU of a lower (L) and an upper (U) triangular matrix generated by a variant of the Crout factorization algorithm: only the elements of $\mathbf{A}$ that are originally non-zero are factorized and stored. In this way the sparsity structure of $\mathbf{A}$ is completely preserved. However, ILU cannot be efficiently implemented on a distributed memory machine. In order to overcome these problems, the BILU preconditioner has been proposed in Stella *et al.* (1993). It is based on a block decomposition of matrix $\mathbf{A}$ with no overlapping among the diagonal blocks: each processor performs an ILU factorization only on a square block centred on the main diagonal. This preconditioner does not affect the final result obtained by using Bi-CGSTAB, even if it could affect the number of iterations required.

The testing of the described numerical model has been extensively discussed in Guj and Stella (1993) and Stella and Bucchignani (1996). The numerical inaccuracies reported in meeting mass conservation and vorticity definition had the same order of magnitude as the round-off error at each time step.

3.2 Time and space mesh sensitivity

The numerical code that we have used here was already validated: in Giangi *et al.* (1998) a good comparison was described versus the solution computed by Behnia and De Vahl Davis in Roux (1990) in the case of the flow here considered at $Pr = 0.015$ and $Gr = 20,000$; in the case of the Rayleigh-Benard problem accurate numerical flows were presented in Bucchignani (1997) and Stella and Bucchignani (1998). Then, for costs reasons, we performed a test for mesh sensitivity just assuming $Gr = 100,000$ with a configuration made up of a large horizontal roll. Three grids have been used: $54 \cdot 14 \cdot 14$, $81 \cdot 21 \cdot 21$ and $131 \cdot 31 \cdot 31$. The maximum values of the three components of velocity and the average Nusselt number in the x direction have been chosen for comparison. As proposed by de Vahl Davis (1983), $\mathbf{u_{max}}$, $\mathbf{v_{max}}$ and $\mathbf{w_{max}}$ are computed by numerical differentiation through a fourth order polynomial approximation, for better evaluation of the maximum values.

Results are reported in Table I. The convergence analysis indicates that the method is nearly second order accurate in space. The grid $81 \cdot 21 \cdot 21$ provides a solution that is accurate enough for the purposes of this paper, so we assumed that it could produce sufficient accuracy also for the other simulations at higher values of Gr.

The time step sensitivity analysis has been executed on a two dimensional problem. The results, reported in Stella and Bucchignani (1996) show that the method is nearly second order accurate in time. This is due to the linearization procedure where the second order correction to velocity and vorticity are neglected.

3.3 Fractal dimension of an attractor

The unsteady flows that we have obtained have been analyzed by means of the nonlinear dynamic technique that is briefly described in the following.

As discussed in Bezé *et al.* (1984), the evolution of a dynamical system can be described by means of a phase trajectory, which is a curve traced in the phase space having as many dimensions as the number of degrees of freedom of the

	$54 \cdot 14 \cdot 14$	$81 \cdot 21 \cdot 21$	$131 \cdot 31 \cdot 31$
$\mathbf{u}_{max}$	1.3175	1.3405	1.3522
x,y,z	2.01 0.25 0.600	2.05 0.227 0.575	2.060 0.233 0.556
$\mathbf{v}_{max}$	0.6960	0.6995	0.7204
x,y,z	0.15 0.500 0.575	0.125 0.400 0.562	0.100 0.350 0.559
$\mathbf{w}_{max}$	0.4395	0.4038	0.3926
x,y,z	0.125 0.700 0.850	0.125 0.675 0.860	0.125 0.675 0.860
Nu	1.6104	1.5992	1.5933

Table I. Mesh sensitivity analysis: Gr = 100,000

system. For dissipative systems, all the trajectories end on a geometrical object called attractor.

The number of dimensions (d) of an attractor provides important information about the kind of temporal regime that characterizes the system under study. In fact, for a periodic regime, the attractor is a closed curve lying in a plane ($d = 1$), for a quasi periodic regime with two incommensurate frequencies the attractor is a toroidal surface ($d = 2$). If the temporal regime is chaotic, the phase trajectories end on a strange attractor, which is characterized by a number of dimensions larger than two and not necessarily integer: the strange attractor is characterized by a fractal dimension.

On the basis of what we said above, it is simple to understand the importance of measuring the dimension of an attractor. A purely geometric measure of the structure of the attractor is supplied by the Hausdorff-Besikovich fractal dimension D: given a set of points in a p-dimensional space, let $N(\epsilon)$ be the smallest number of hypercubes (of size ϵ) needed to cover this set; D is defined as:

$$D = \lim_{\epsilon \to 0} \frac{\ln N(\epsilon)}{\ln(1/\epsilon)}$$

However, D is difficult to calculate and impracticable for high dimensional systems. For this reason the evaluation of the correlation dimension ν has to be preferred; it is related to D by the inequality $\nu \leq D$. In this work the procedure proposed by Grassberger and Procaccia (1983) has been chosen, because it yields accurate values, but it is not very heavy from a computational point of view. This procedure can be summarized as follows:

(1) given a set of points lying on an attractor in the pseudo-phase space[1], let $N(r)$ be the number of points located in a hyper-sphere of radius r: it is $N(r) \propto r^{\nu}$;

(2) let us introduce the correlation function:

$$C(r) = \lim_{m \to \infty} \frac{1}{m^2} \sum_{ij} H(r - |\bar{x}_i - \bar{x}_j|)$$

in which H is the Heaviside function, defined in such a way that $H = 1$ if its argument is positive, 0 otherwise. In this way the sum indicates the number of couples of points whose mutual distance is less than r. It can be shown that:

$$C(r) \propto N \propto r^{\nu}$$

(3) once the curve $C(r)$ has been traced in the plane$(\log C, \log r)$, the slope of it approximately yields the value of ν. As the dimension p of the pseudo-phase space is not known a priori, it is necessary to trace the curve $C(r)$ for several values of p, increasing p until the value of ν does not change more than p. If, as p grows, it results:

- $\nu \to 1$: the signal is periodic;
- $\nu \to 2$: the signal is quasi-periodic with two frequencies;
- $\nu \to k$ (k is a real number larger than 2): the signal is chaotic (deterministic chaos);
- ν always growing with p: the signal is random (white noise).

4 Results

The numerical simulations have been executed in double precision on the SGI Power Challenge super computer, installed in CIRA. It is a shared memory multiprocessor machine with 4GB of physical memory and with 16 R10000 processors. A computational grid with $81 \cdot 21 \cdot 21$ points ($\Delta x = \Delta y = \Delta z = 0.05$) has been chosen, while the time step has been set equal to 10^{-5}, as a good compromise between time accuracy and computational resources. The Prandtl number has been set equal to 0.015, while the Grashof number has been varied in order to observe a series of transitions and bifurcations as this parameter is increased. The following nomenclature has been adopted in order to characterize the various temporal regimes:

- S: steady state;
- P: periodic regime with one fundamental frequency;
- QP_2: quasi-periodic regime with two incommensurate frequencies;
- QP_3: quasi-periodic regime with three incommensurate frequencies;
- N: chaotic regime.

We have established the steady states by computing the Euclidean norm of the relative difference of the velocity vectors at two consecutive time steps. The chosen tolerance was 10^{-4}. Furthermore, steady solutions have been randomly perturbed (small perturbations) in order to check for stability.

Table II contains a summary of the most significant solutions obtained as a function of the Grashof number. For the unsteady solutions, the quantities reported in the table have been averaged over a long time interval. The first

Gr	Regime	$\mathbf{u}_{max}$	$\mathbf{v}_{max}$	$\mathbf{w}_{max}$	$\mathbf{Nu}_x$
100,000	S	1.3405	0.6995	0.4038	1.5992
200,000	S	1.3863	0.7001	0.4066	2.1476
205,000	P	1.3864	0.7013	0.4067	2.1704
206,000	QP_2	1.3865	0.7015	0.4067	2.1717
207,000	QP_2	1.3865	0.7016	0.4067	2.1795
210,000	QP_2	1.3867	0.7021	0.4069	2.1929
215,000	QP_3/N	1.3892	0.7759	0.5092	2.2104
220,000	N	1.3913	0.8596	0.5188	2.2362
240,000	N	1.3867	0.8865	0.6650	2.2461
300,000	N	1.4171	0.9082	0.6242	2.5183

Table II. Configuration, regime, maximum values of the three velocity components, Nusselt number in the middle plane normal to the x axis

simulation has been executed at $Gr = 100,000$ starting from rest: a steady solution, made up of a large horizontal roll (one-roll) has been found. Figure 2 shows the profile along y ($x = 2, z = 0.5$) of the u velocity component and the profile along x ($y = 0.5, z = 0.5$) of the v velocity component. Figure 3 shows the iso-u in the z-normal middle plane.

The second simulation has been executed at $Gr = 200,000$, starting from the solution obtained at $Gr = 100,000$. Figure 4 shows the time history related to the u velocity component at the point $(0.4, 0.75, 0.4)$: after a finite time interval (0.4 non-dimensional units), the flow becomes steady.

The next simulation has been executed at $Gr = 205000$: as shown in Figure 5, after a finite time interval the flow becomes steady again. However, a small random perturbation given on the vorticity field highlights that this is a false steady state: in fact, after the perturbation, the flow becomes oscillatory periodic with one fundamental frequency $f_1 = 11.104$ (Figure 6), which is accompanied by two harmonics ($f_2 = 3 \cdot f_1, f_3 = 5 \cdot f_1$).

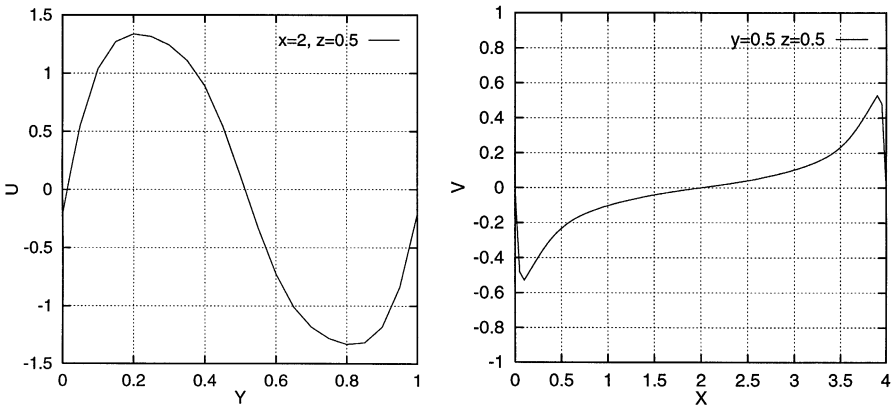

Figure 2.
Case at Gr = 100,000: (left) profile along y (x = 2, z = 0.5) of the u velocity component, (right) profile along x (y = 0.5, z = 0.5) of the v velocity component

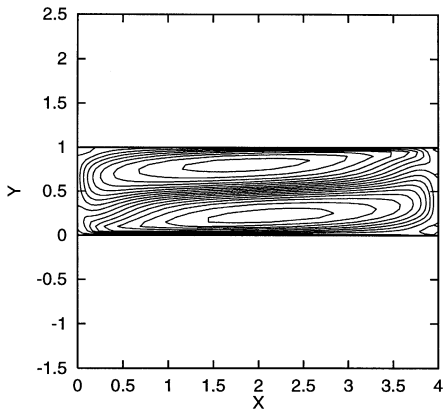

Figure 3.
Case at Gr = 100,000: iso-u in the z-normal middle plane

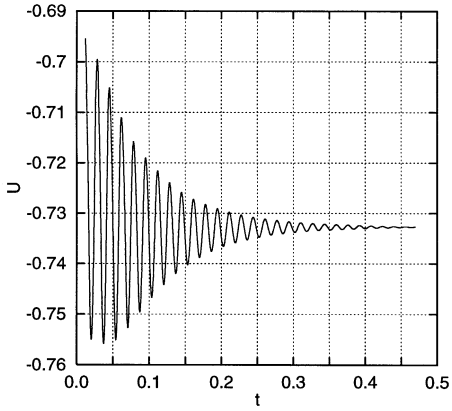

Figure 4.
Case at Gr = 200,000: time history of the u velocity component at the point (0.4, 0.75, 0.4)

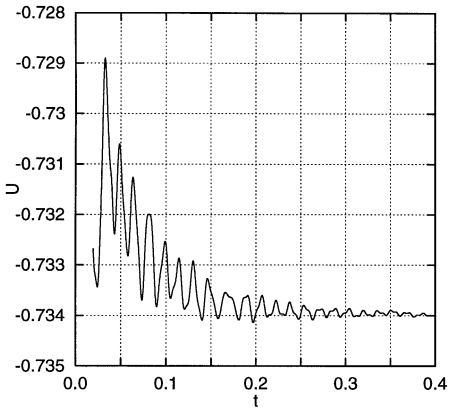

Figure 5.
Case at Gr = 205,000: time history of the u velocity component at the point (0.4, 0.75, 0.4) in the first time interval (0-0.4)

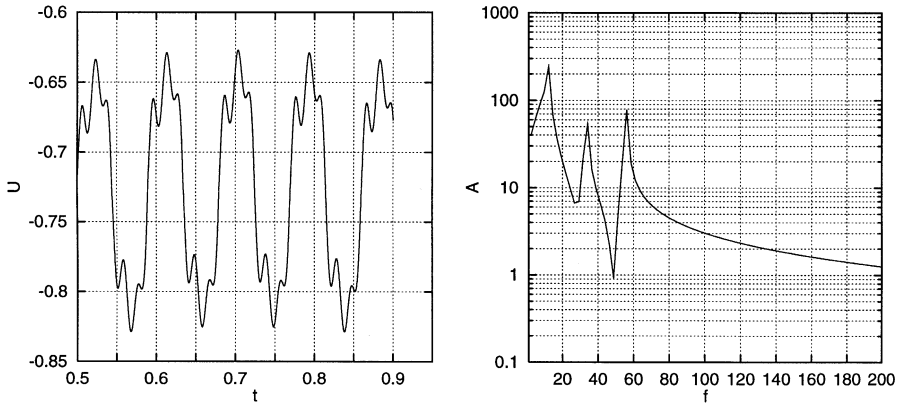

Figure 6.
Case at Gr = 205,000: (left) time history of the u velocity component at the point (0.4, 0.75, 0.4) in the second time interval (0.4-0.9), after the perturbation, (right) FFT of this signal. A periodic regime with a fundamental frequency is observed

An increase in Gr at 206,000 causes the second Hopf bifurcation with a transition to a quasi-periodic regime with two incommensurate frequencies. Figure 7 shows the time history of the u velocity component at the point

$(0.4, 0.75, 0.4)$ related to the time interval $0 - 0.6$ (60,000 samples are available). In order to perform a Fourier analysis, this signal has been "filtered" considering only 12,000 samples (one every five). A FFT executed on the last 2^13 samples (time interval $[0.1994, 0.6]$ highlights the presence of two main frequencies ($f_1 = 12.207$ and $f_2 = 51.269$) accompanied by a large number of harmonics. An analysis of the flow configuration shows that the one-roll configuration is partially destroyed (Figure 8) only for a limited time interval $(0.15, 0.2)$, but it is preserved successively. The flow remains quasi-periodic even at $Gr = 207,000$ and at $Gr = 210,000$, with slightly different values of the main frequencies. We observe that the first main frequency increases its value, while the second one decreases as Gr grows (Table III).

At $Gr = 215,000$ a transition to a chaotic regime is observed. However, this is not a direct transition and the presence of a quasi-periodic regime with three incommensurate frequencies has been observed during the initial stage of this simulation. As shown in Figure 9, the FFT executed on the time history of the u velocity component highlights the presence of a third fundamental frequency ($f_1 = 18.310, f_2 = 42.724, f_3 = 67.138$). However, a broadband noise, typical of

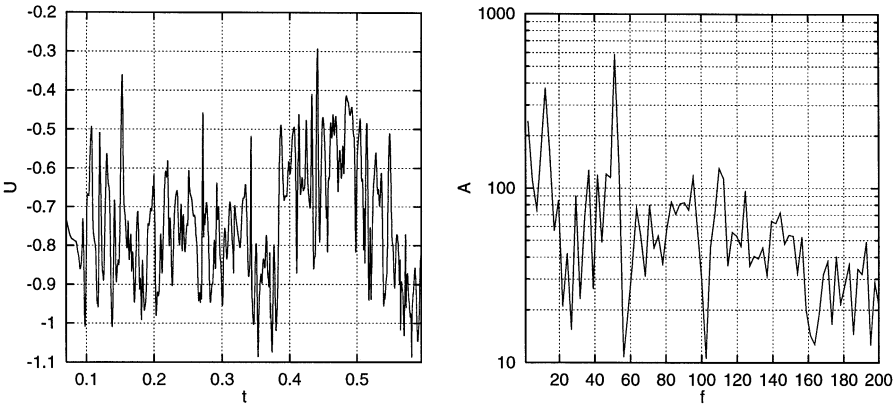

Figure 7.
Case at Gr = 206,000: (left) time history of the u velocity component at the point (0.4, 0.75, 0.4), (right) FFT of this signal. A quasi-periodic regime with two incommensurate frequencies is observed

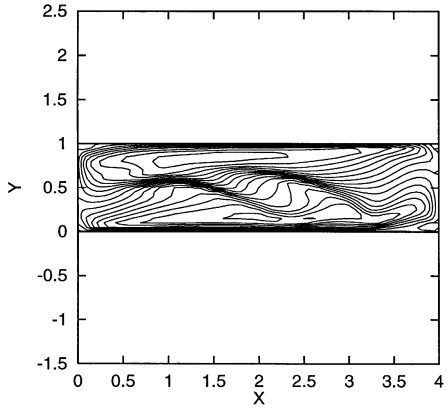

Figure 8.
Case at Gr = 206,000: iso-u in the z-normal middle plane at t = 0.15

the chaotic systems, is also observable. As explained in section 3.3, a better characterization of the signal can be achieved by evaluating the fractal dimension of the attractor. Figure 10 shows the curves traced in the plane $(\log C(r), \log r)$ for increasing values $(p = 2, 3, 4 \ldots)$ of the embedding dimension of the pseudo-phase space. The time delay τ has been set equal to $100 \cdot \Delta t$. We can observe that the slope of the curves tends to become independent on p and to stabilize on the value 3.72. This means that we are dealing with a strange attractor.

Further increases in Gr, up to 300,000, do not cause significant changes in the temporal regime, which remains chaotic. Figure 11 shows the iso-u in the z-normal middle plane: a not regular fluid dynamics configuration can be observed.

In conclusion, the bifurcation sequence observed is the following:

$$S \rightarrow P \rightarrow QP_2(\rightarrow QP_3) \rightarrow N$$

This is the well known Ruelle-Takens route, which has been already the subject of theoretical as well as practical investigations. The present results allow us to conclude that the Newhouse-Ruelle-Takens theorem (Newhouse *et al.*, 1978) is valid for the present problem; this theorem asserts that a torus T^3, under the actions of some perturbations, degenerates to a strange attractor and therefore the existence of three frequencies (i.e. three degrees of freedom) is a necessary and sufficient condition for the onset of a chaotic regime. Other results agreeing with these conclusions are shown in Guzman and Amon (1996) and

Gr	f_1	f_2	f_1/f_2
206,000	12.207	51.269	4.199
207,000	13.573	49.846	3.672
210,000	17.089	43.945	2.571

Table III. Quasi-periodic regime QP_2: main frequencies and their ratio

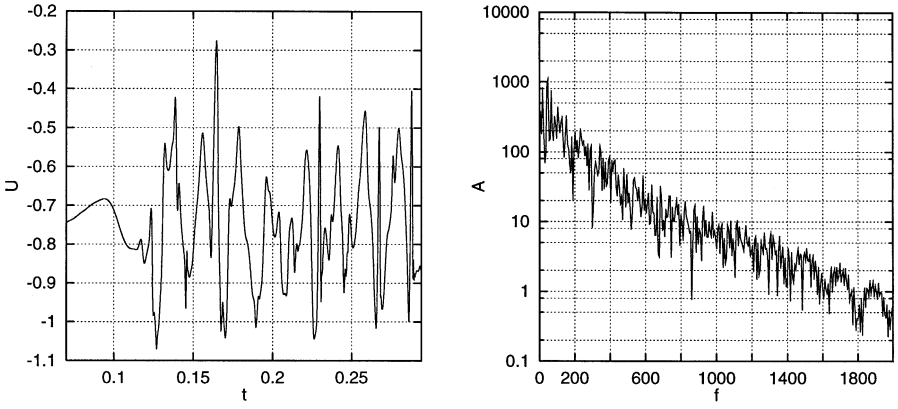

Figure 9. Case at Gr = 215,000: (left) time history of the u velocity component at the point (0.4, 0.75, 0.4), (right) FFT of this signal. The power spectrum highlights a non-periodic state with relatively sharp peaks just above the onset of noise

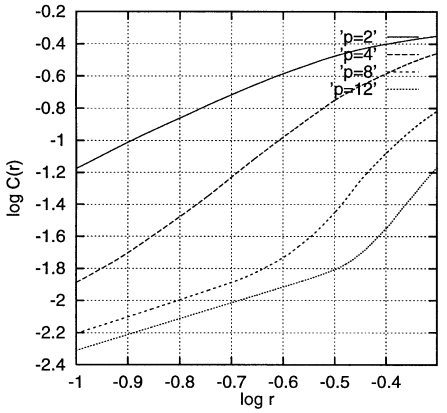

Figure 10.
Case at Gr = 215,000: evaluation of the fractal dimension of the attractor

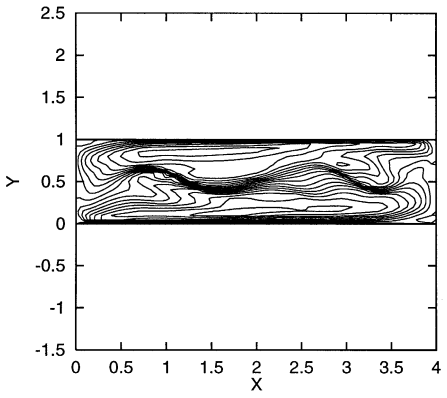

Figure 11.
Case at Gr = 30,000: iso-u in the z-normal middle plane

Bucchingnani and Stella (1998); on the other side, Gollub and Benson (1980), in the Rayleigh-Benard convection, observed a stable three periodic regime for a finite range of values of the control parameter (i.e. the Rayleigh number).

Conclusions

A numerical study of the unsteady horizontal thermal convection has been executed. The physical system considered is a liquid metal ($Pr = 0.015$) in a three-dimensional box $4 \cdot 1 \cdot 1$ with a different temperature at the furthest vertical walls.

Because many applications of material science, metereology, geology and others are governed or strongly affected by this kind of flow, we think that it deserves as much attention as its vertical counterpart, the Benard convection. From the scientific viewpoint, we think that the last one has received much more attention so far due to the possibility of starting the study from the easy conduction state, that is a stable flow for sufficiently low Grashof numbers. In fact in the literature, for the physical system considered here, we find a good amount of mathematical and numerical results in the two-dimensional case

(just to mention some of them: Roux (1990); Winters (1988); Pulicani *et al.* (1990)); in three dimensions we know only a few published works on mathematical treatments within restrictive hypothesis (Cormack *et al.,* 1974; Gershuni *et al.,* 1992; Georgescu and Mansutti, 1998; 1999) and on numerical simulations (Mundrane and Zebib, 1993; Behnia *et al.*, 1995; Giangi *et al.,* 1998). The goal of this work is the analysis of the transition from the steady flow to the oscillatory periodic regime and the successive transition to chaos.

The study of this phenomenon requires a huge amount of computational work and parallel computing resources: actually the transient regimes are very lengthy and the resolution of the nonlinearities in the equations needs high accuracy. In the present work the use of a parallel fully implicit approach allowed us to obtain a significant quantity of numerical data in a reasonable time.

We have considered the one-roll flow configuration and have detected three Hopf bifurcations: the first one from steady to periodic regime with one frequency at $Gr = 205,000$, the second one from periodic to quasi-periodic regime with two incommensurate frequencies at $Gr = 206,000$ and the third one from quasi-periodic with two frequencies to quasi-periodic with three frequencies at $Gr = 215,000$. The last regime being quite unstable rapidly degenerates to chaos. A quantitative characterization of the chaotic regime has been attained evaluating the fractal dimension of the attractors. In this bifurcation sequence we recognize the Ruelle-Takens route to chaos, which has already been observed in other physical systems, both numerically and experimentally.

Comparing with the results in literature on the two-dimensional case, we stress a significant difference: in two dimensions as Gr increases the flow undergoes hysteresis cycle according to which the flow regime changes from steady to periodic to quasi-periodic to steady again (Pulicani *et al.*, 1990; Muller and Neumann, 1983); in three dimensions we see the flow regime changing from steady to periodic to quasi-periodic to chaotic. Such a difference suggests that the three-dimensional effects are not at all negligible and the two-dimensional studies seem to have a scarce applicability within real three-dimensional problems.

As future work we shall slightly modify the physical system studied here and consider an open top cavity with thermocapillary effects at the fluid/air interface. The resulting flow is of interest for applications in microgravity environments.

Note

1. For a scalar time series $x(t_k)(t_k = k \cdot \Delta t)$ the state vectors in the pseudo-phase space are given by

$$F(t_k = \{x(t_k, x(t_k + \tau), x(t_k + 2\tau) \ldots x(t_k + (p-1)\tau)\}$$

in which τ is the time delay that is a multiple of $\Delta t.\tau$ is chosen by the first zero of the autocorrelation function and the embedding dimension p is increased until the invariant property (fractal dimension) does not change.

References

Behnia, M., Stella, F. and Guj, G. (1995), "A numerical study of three-dimensional low *Pr* buoyancy and thermocapillary convection", *Numerical Heat Transfer Part A*, Vol. 27, pp. 73-88.

Ben Hadid, H. and Roux, B. (1990), "Thermocapillarity convection in long horizontal layers of low-Prandtl-number melts subject to a horizontal temperature gradient", *Jour. Fluid Mech.*, Vol. 221, pp. 77-103.

Bergé, P., Pomeau, Y. and Vidal, C. (1984), *Order Within Chaos – Towards a Deterministic Approach to Turbulence*, John Wiley & Sons, New York, NY.

Bucchignani, E. (1997), "Convezione di Rayleigh-Benard nonstazionaria in domini limitati. Transizione al caos", PhD thesis, Universitá di Roma "La Sapienza".

Bucchignani, E. and Stella, F. (1995), "A fully implicit parallel solver for viscous flows: numerical tests on high performance machines", in Ecer, A. *et al.* (Ed.), *Parallel Computational Fluid Dynamics: Implementations and Results Using Parallel Computers*, Elsevier, Amsterdam, pp. 569-76.

Bucchignani, E. and Stella, F. (1998), Rayleigh-Bénard convection in limited domains: Part 2 – transition to chaos", *Num. Heat Tr. Part A*.

Cormack, D.E., Leal, L.G. and Imberger, J.J. (1974), "Natural convection in a shallow cavity with differentially heated end walls. Part 1. Asymptotic theory", *Jour. Fluid Mech.*, Vol. 65 No. II, pp. 209-19.

de Vahl Davis, G. (1983), "Natural convection of air in a square cavity: a benchmark numerical solution", *Int. J. Num. Meth. Fluids*, Vol. 3, pp. 249-64.

Drazin, P.G. and Reid, W.H. (1985), "Hydrodynamic stability", *Cambridge Monographs on Mechanics and Applied Mathematics*.

Georgescu, A. and Mansutti, D. (1998), "A finite dimensional approach for the horizontal convection", submitted for publication in *Int. Jour. Nonlinear Mech.*

Georgescu, A. and Mansutti, D. (1999), "Coincidence of the linear and nonlinear stability bounds in a horizontal thermal convection problem", *Int. Jour. Nonlinear Mech.*, Vol. 34 No. 4, pp. 603-13.

Gershuni, G.Z., Laure, P., Myznikov, V.M. Roux, B. and Zhukhovitsky, E.M. (1992), "On the stability of plane-parallel advective flows in long horizontal layers", *Microgravity Quar.*, Vol. 2, pp. 141-51.

Giangi, M., Mansutti, D. and Richelli, G. (1998), "Steady 3D flow configurations for the horizontal thermal convection with thermocapillary effects", accepted for publication in *Jour. Scient. Computing*.

Gollub, J.P. and Benson, S.V. (1980), "Many routes to turbulent convection", *J. Fluid Mech.*, Vol. 100, pp. 449-70.

Grassberger, P. and Procaccia, I. (1983), "Characterization of strange attractors", *Phys. Rev. Lett.*, Vol. 50, pp. 346-9.

Guj, G. and Stella, F. (1993), "A vorticity-velocity method for the numerical solution of 3D incompressible flows", *J. Comput. Phys.*, Vol. 106, pp. 286-98.

Guzman, A.M. and Amon, C.H. (1996), "Dynamical flow characterization of transitional and chaotic regimes in converging-diverging channels", *J. Fluid Mech.*, Vol. 321, pp. 25-57.

Harlor, F. and Welch, J. (1965), "Numerical calculation of time dependent viscous incompressible flow of fluid with free surface", *Physics of Fluids*, Vol. 8, p. 2182.

Hart, J.E. (1972), "Stability of thin non-rotating Hadley circulations", *J. Atmos. Sci.*, Vol. 29, pp. 687-96.

Hung, M.C. and Andereck, C.D. (1990), "Subharmonic transitions in convection in a moderately shallow cavity", *Notes on Num. Fluid Mech.*, Vol. 27, Vieweg Publishers, pp. 338-43.

Hurle, D.T.J. (1983), "Convective transport in melt growth systems", *J. Crystal Growth*, Vol. 65, pp. 124-32.

Hurle, D.T.J., Jakeman, E. and Johnson, C.P. (1974), "Convective temperature oscillations in molten gallium", *J. Fluid Mech*., Vol. 64, pp. 565-76.

Lebon, G. (1984), "Recent developments in surface-tension driven instabilities", *Acta Astronautica*, Vol. 11, pp. 353-9.

Lorenz, E.N. (1963), "Deterministic non-periodic flow", *J. Atmosph. Sciences*, Vol. 20, p. 130.

Muller, G. and Neumann, G. (1983), *Jour. Cry. Growth*, Vol. 63, pp. 58-88.

Mundrane, M. and Zebib, A. (1993), "Two- and three-dimensional buoyant thermocapillary convection", *Phys. Fluids A*, Vol. 5, pp. 810-18.

Newhouse, S., Ruelle, D. and Takens, T. (1978), "Occurrence of strange axiom-A attractors near quasi-periodic flows on T^m, $m \geq 3$", *Commun. Math. Phys*., Vol. 64, p. 35.

Pulicani, J.P., Crespo, E., Randramampianina, A., Bontoux, P. and Peyret, R. (1990), "Spectral simulation of oscillatory convection at low Prandtl number", *Int. J. Num. Meth. Fluids*, Vol. 10, pp. 481-517.

Roux, B. (Ed.) (1990), "GAMM-Workshop on numerical simulation of oscillatory convection in a low *Pr* fluid", Marseille, France, October 1988, published as Notes on *Num. Fluid Mech*., Vol. 27, Vieweg Publishers.

Stella, F. and Bucchignani, E. (1996), "True transient vorticity-velocity method using preconditioned Bi-CGSTAB", *Numerical Heat Transfer Part B*, Vol. 30, pp. 315-39.

Stella, F. and Bucchignani, E. (1998), "Rayleigh-Bénard convection in limited domains: Part 1 – oscillatory flow", *Num. Heat Tr. Part A*.

Stella, F., Marrone, M. and Bucchignani, E. (1993), "A parallel preconditioned CG type method for incompressible Navier-Stokes equations", in Ecer, A. *et al.* (Ed.), *Parallel Computational Fluid Dynamics: New Trends and Advances*, Elsevier, Amsterdam, pp. 325-32.

van der Vorst, H. (1992), "Bi-CGSTAB, a fast and smoothly converging variant of Bi-CG for the solution of nonsymmetric linear systems", *SIAM J. Sci. Stat. Comput*., Vol. 13 No. 2, pp. 631-44.

Wang, T.M., Korpela, S.A., Hung, M.C. and Andereck, C.D. (1990), "Convection in a shallow cavity", *Notes on Num. Fluid Mech*., Vol. 27, Vieweg Publishers, pp. 344-53.

Winters, K.H. (1988), "Oscillatory convection in liquid metals with a horizontal temperature gradient", *Int. Jour. Num. Meth. Engrng*., Vol. 25, pp. 401-14.